JOURNAL OF CATALYSIS 106, 500–511 (1987)

ENDOR of Perylene Radicals Adsorbed on Alumina and Silica–Alumina Powders. I. The Ring Protons

R. B. CLARKSON, R. L. BELFORD, K. S. ROTHENBERGER, AND H. C. CROOKHAM

Department of Chemistry and the Illinois ESR Research Center, University of Illinois, Urbana, Illinois 61801

Received January 6, 1986; revised March 17, 1987

Complex electron-nuclear double-resonance (ENDOR) spectra were obtained from the radicals formed on activated alumina and silica–alumina powders exposed to solutions of perylene in benzene. Use of deuterated solvent to suppress spectral contributions from proton matrix effects enabled more detailed analysis of resonances associated with hyperfine interactions of ring protons of the perylene radical ion. A model of isotropic Zeeman interactions (g) and very anisotropic hyperfine splittings (A) is supported by multifrequency EPR measurements and ENDOR simulations devised for this work. All three proton hyperfine interactions of the perylene radical ion were resolved and the absolute values of the principal elements of the hyperfine coupling matrices were obtained. The fact that these values for radicals formed on alumina and silica–alumina were nearly identical implies that the same radical species forms on both surfaces. These findings are discussed and the radical is assigned as the cation.

1. INTRODUCTION

1.1. Historical background. It is well established experimentally that stable adsorbed free radicals form on activated alumina and silica–alumina powders exposed to solutions of perylene in benzene (*1–3*). Dollish and Hall showed that the extent of radical formation depended on the amount of oxygen taken up by the system, as well as on the presence of dehydroxylated sites at the surface, and suggested that the radical formed in the process is perylene cation (*4*). Muha (*5–7*) and Flockhart *et al.* (*8, 9*) have investigated the system in considerable detail.

Several aspects of these surface reactions remain controversial, including the original assignment of the radical, the mechanism of its formation, and the means by which hyperfine structure in its electron paramagnetic resonance (EPR or ESR) spectrum sometimes is obscured. Muha has suggested that it is the perylene anion radical that forms on activated alumina while the cation radical forms on silica–alumina surfaces (*10*). Flockhart and Salem suggest that the cation is the primary species on both surfaces, but that over time, oxygen adds to the radical on alumina, forming an aryloxy radical (*11*). This new species is expected to retain little of the symmetry of its precursor perylene cation; all 11 of its protons would be magnetically different, whereas its precursor would have only 3 distinct types of protons. The resulting hyperfine pattern could be sufficiently complex to destroy resolution of the proton structure often observed in the EPR spectra of such samples. Wozniewski *et al.* (*12*), on the other hand, postulate formation of two cation species, one by electron transfer (Lewis acid sites) and the other by hydrogen addition (Brønsted acid sites). They argue that surface attachment of the radicals to aluminum atoms at Lewis acid sites creates a species having particularly low symmetry and thus complex, poorly resolved hyperfine structure.

One of the difficulties surrounding the EPR study of the perylene radical on metal oxide substrates has been that even under the best conditions, poor resolvability of the EPR spectrum has prevented definitive extraction of (1) the smallest (β) coupling constant (*5, 9*) and (2) the hyperfine aniso-

0021-9517/87 $3.00

tropies. Such uncertainties in the details of proton hyperfine interactions in the adsorbed radical are unfortunate, particularly in the light of current debate on the nature of the radical species formed in this system, because a more complete experimental determination of the hyperfine coupling matrices should provide valuable clues to species assignment. Moreover, to the extent that some of the proton hyperfine coupling parameters are measurably sensitive to environmental effects such as interactions with the surface, counter-ions, and other radicals (*13, 14*), a means to measure all the anisotropic coupling constants should not only help with the characterization but also shed some light on the mechanism of formation.

In an effort to learn more about perylene/alumina and perylene/silica–alumina chemistry, we performed electron-nuclear double-resonance (ENDOR) spectroscopy on the systems. This paper focuses on the anisotropic proton hyperfine interactions, which are useful in the elucidation of molecular structure. Here we report (1) the resolution of all three of the proton hyperfine interactions of the adsorbed perylene radical, (2) successful simulation of the proton ENDOR spectra using a modified form of the theory of Dalton and Kwiram (*15*), and (3) the resulting diagonal elements of the anisotropic hyperfine matrices for each interaction. This evidence suggests strongly that the perylene radical species formed on activated alumina and silica–alumina powders is the same and that it is the cation. In addition, we observed the interaction of the aromatic radicals with protons associated with the solvent and with the surface, and also with ^{27}Al nuclei on the surface; these data will be reported and interpreted in a subsequent paper dealing with intermolecular spin interactions.

1.2. The spectroscopic techniques. EPR spectroscopy has proven to be a very useful tool in the study of radicals formed on active metal oxide surfaces (*16*). The technique has excellent sensitivity, and analysis of hyperfine structure in the spectra can be a route to species identification. For a radical having one unpaired electron and many magnetic ($I \neq 0$) nuclei, the EPR spectrum typically consists of many electron spin transitions, each subject to the *simultaneous* influence of (i.e., hyperfine interaction with) *all* the magnetic nuclei in the system. Consequently, one often observes an exceedingly complex spectrum of many nearly overlapping resonance lines. Since inhomogeneous line-broadening often limits resolution, such a complex spectrum may not be resolved, and information may be obscured. On the other hand, the ENDOR spectrum typically consists of several *single*-nucleus spin transitions, each subject to the influence of (i.e., hyperfine interaction with) the electron. Thus one may observe a much simpler spectrum. This fact, coupled with an inherent linewidth reduction (*17*), can result in ENDOR resolution of weak hyperfine interactions that are unresolved in EPR.

The EPR spectrum of a hydrocarbon such as the perylene radical is customarily described in terms of a spin Hamiltonian:

$$H_S = \sum_i \beta \mathbf{S}_i \cdot \mathbf{g} \cdot \mathbf{B}(t) - \sum_k \beta_n \mathbf{I}_k \cdot \mathbf{g}_{nk} \cdot \mathbf{B}(t) + \sum_i \sum_k \mathbf{S}_i \cdot \mathbf{A}_{ik} \cdot \mathbf{I}_k + H_{SS} + H_{SL} + H_{IL} + H_L. \quad [1]$$

In this equation, which is the meeting ground between a mathematical model for the system and the experimental spectral data, the first term describes the interaction of the unpaired electronic spins $\{\mathbf{S}_i\}$ with the dc and high frequency magnetic field $\{\mathbf{B}(t)\}$, the second describes a similar interaction between nuclei with nonzero spins $\{\mathbf{I}_k\}$ and the external field, and the third accounts for the electron-nuclear hyperfine interactions. Interactions of the electron spins with each other (H_{SS}), electron spin–lattice interactions (H_{SL}), nuclear spin–

lattice interactions (H_{IL}), and lattice energy (H_L) are assumed to be small or constant contributions to the energy of the system and will henceforth be neglected.

In the case of polycyclic aromatic radicals, spectral information related to molecular structure and environment is contained in each term of the Hamiltonian, but the hyperfine terms are especially useful in characterizing a particular species. A perylene radical formed by the loss or addition of an electron has at least three chemically distinct types of ring protons. Characterization of its hyperfine interactions thus requires at least three independent coupling matrices **A**. In addition, there will be electron-nuclear dipole–dipole interactions between the unpaired electrons and nonbonded nuclei with spin (e.g., ^{1}H, ^{13}C, and ^{27}Al). The intramolecular proton hyperfine interactions are responsible for the fine structure seen in the EPR spectra of aromatic hydrocarbon radicals formed on activated metal oxide surfaces.

The *orientation dependences* of the Zeeman and internal interactions of the radical are described by the coupling matrices **g**, $\mathbf{g}_n$, and $\mathbf{A}_{ik}$'s in Eq. [1]. In the case of many polycyclic aromatic hydrocarbon radicals, **g** and $\mathbf{g}_n$ are so nearly isotropic that we may write them as scalar constants. Roughly speaking, each matrix, $\mathbf{A}_{ik}$, carries the information on the variation of the hyperfine coupling between I_k and S_i as a function of the orientation of the external magnetic fields, B_0, relative to the line of centers of the I_k, S_i interaction pair. Then, for a simple system comprised of a single electron and proton ($S = \frac{1}{2}$, $I = \frac{1}{2}$) at a high field strength where the electronic Zeeman interaction dominates, Eq. [1] can be approximated by a simpler form:

$$H_S = g\beta B_0 S_{z'} - g_n\beta_n B_0 I_{z'} + hS_{z'}(A_{z'x'}I_{x'} + A_{z'y'}I_{y'} + A_{z'z'}I_{z'}). \quad [2]$$

Here, x', y', z' are laboratory axes. If more than one nuclear spin is involved in the molecule, then an additional hyperfine term must be written for each magnetically unique nucleus. In addition, other terms resulting from the general **I**,**S** interactions may need to be included. Foremost among these is the through-space dipole–dipole interaction between the unpaired electron and more distant, nonbonded nuclei. We shall see that it also can provide us with important information in the study of metal oxide surfaces. A Hamiltonian of the form given in Eq. [2] results in a set of magnetic spin energy levels like that shown in Fig. 1.

Because the samples most often encountered in the study of heterogeneous catalysis are powders, all orientations of the molecular system relative to the external magnetic field contribute to the observed EPR spectra. If **g** and/or **A** terms are anisotropic, the resulting composite, commonly called a "powder spectrum," can contain

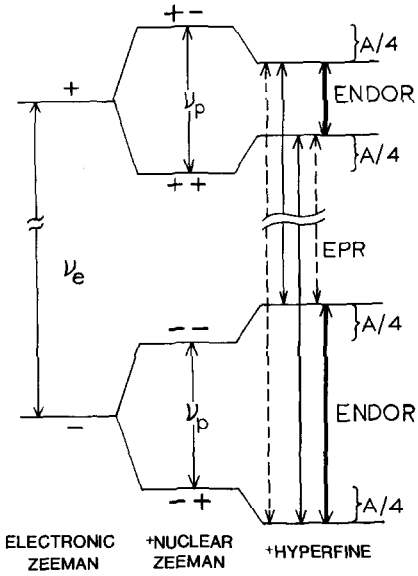

FIG. 1. Simplified (first-order) diagram of energy levels and transitions for one unpaired electron and one proton in magnetic field, B_0. States labeled according to signs of M_S and M_I (e.g., − + means $M_S = -\frac{1}{2}$; $M_I = +\frac{1}{2}$). Energy terms are (1) *e*lectron Zeeman ($E_{eZ} = g\beta B_0 M_S \equiv \nu_e M_S$), (2) *n*uclear Zeeman ($E_{nZ} = -g_n\beta_n B_0 M_I \equiv -\nu_p M_I$), and (3) *hyperfine* interaction ($E_{hfi} \approx hAM_SM_I$). Transitions shown: two primary ("allowed") EPR (—); two secondary ("forbidden") EPR (---); two ENDOR ($f_{ENDOR} = |\nu_p \pm A/2|$) (—).

very broad and asymmetric lines. This fact, coupled with the complex pattern of transitions found in the EPR spectra of molecules like perylene and in the presence of other mechanisms such as heterogeneous sample environment (which gives rise to inhomogeneous line-broadening that increases observed linewidths), may cause spectral features such as the weak β-proton hyperfine contribution to the cw EPR spectra of many radicals formed on alumina and silica–alumina surfaces to be unresolved. The information about molecular structure found in the hyperfine interactions, $\mathbf{A}_{ik}$, thus may be lost in the EPR spectra of disordered solids (powders, polycrystalline samples, glasses). Also, information on the environment of the radical found in the even weaker dipole–dipole interactions is extremely difficult to deduce from such EPR measurements, since linewidths and lineshapes, which often are the reflection of such interactions in conventional spectra, are now potentially influenced by so many factors, making modeling of the lineshape a very difficult and uncertain calculation.

The ENDOR technique is described by Kevan and Kispert (*17*). The following points are important for the discussion here: (1) ENDOR improves the resolution of inhomogeneously broadened lines in disordered solid samples by probing the *homogeneous* spin packet substructure (a resolution enhancement of $\sim\mu_e/\mu_n$, i.e., about 660 for protons); (2) as mentioned in Section 1.2, ENDOR spectra can be much simpler than EPR spectra since they involve mainly single-nucleus effects; and (3) in solids, ENDOR gives us information on the anisotropic as well as the isotropic part of the hyperfine interaction. As implied by Fig. 2, the typical isotropic proton ENDOR spectrum consists of pairs of resonance lines positioned symmetrically about the Larmor precessional frequency for protons, $\nu_p = g_n\beta_n B_0$,

$$f_{\text{ENDOR}} = |\nu_p \pm A/2|, \qquad [3]$$

where A is defined (cf. Eq. [2]) as

$$A \equiv \{(A_{z'x'})^2 + (A_{z'y'})^2 + (A_{z'z'})^2\}^{1/2}. \qquad [4]$$

For ENDOR spectra of radicals in solution, the rapid tumbling of the molecules usually averages out the anisotropic portion of the hyperfine interaction, producing an isotropic spectrum consisting of a pair of resonance lines for each interaction. In solids, all the information of the anisotropic portion of the interaction is retained in the powder spectrum, producing a much more complex and informative pattern, which must be analyzed by means of a mathematical model or simulation. Such analysis can, as we see in the next section, provide very detailed information about the molecular structure of the radical being observed by obtaining from the experimental data the absolute values of the principal elements of the hyperfine interaction matrix, which are $|A_x|$, $|A_y|$, and $|A_z|$. If the molecule contains several magnetically inequivalent protons, the combination of experiment and theory could obtain the important elements of each hyperfine interaction. For the case of polycyclic aromatic hydrocarbon radicals on surfaces such as alumina and silica–alumina, we successfully made such measurements and analysis, as also discussed in the next section.

In addition to hyperfine interactions between the unpaired electron and nuclei chemically bonded to it in the molecule, there are also electron-nuclear dipole–dipole interactions between the electron and the more distant nuclei. These give rise to an effect called distant or matrix ENDOR, which is manifested by the appearance of additional ENDOR resonance lines located at the nuclear Larmor frequency (*18*). Matrix ENDOR lines, some of which are evident in spectra reported in this paper, can provide much useful information about the adsorption sites experienced by radicals formed on catalytic surfaces and will be the subject of a subsequent paper.

2. EXPERIMENTAL SECTION

2.1. Sample preparation. Aluminum oxide (Baker, "acid washed, suitable for

chromatographic use") and silica–alumina catalyst (Houdry M-46) were activated by calcining an approximately 200-mg sample at 550°C for 12 to 24 h in air in an open quartz glass EPR sample tube (4 mm o.d.). The oxide sample tubes were sealed with septum caps while hot and allowed to cool briefly.

Perylene (Aldrich, Gold Label) was used without further purification and was dissolved in benzene (Fisher, certified ACS reagent grade) or d_6-benzene (Aldrich, 99+ at%) at the concentrations given. Approximately 0.5 ml of each solution was injected by syringe through the septum caps onto the cooled oxide. To evenly distribute the solution on the substrate, care was taken to drive the syringe needle to the very bottom of the sample tube before injection began. Samples thus prepared were white after calcining and turned a uniform deep purple color upon injection of the perylene solution. Unless otherwise indicated, spectra were run within 6 h of sample preparation.

Samples for *Q*-band EPR were prepared in an analogous manner with 1-mm-o.d. quartz tubes and proportionally smaller sample sizes.

2.2. Spectroscopy. *X*-band EPR spectra were obtained on Bruker ER-200D, Bruker ER-220D, and Varian E-9 EPR spectrometers. *Q*-band and *L*-band EPR spectra were recorded on a Varian E-line Century Series 16-in. spectrometer magnet and console with a Varian E-110 (*Q*-band) microwave bridge or a locally constructed *L*-band microwave bridge. All spectrometers were equipped with liquid nitrogen variable temperature accessories for low temperature operation.

The ENDOR spectra were run on a Bruker ER-200D *X*-band EPR spectrometer equipped with an EN 810 ENDOR accessory and an Aspect 2000 computer for spectrometer control and data collection. A 12.5-kHz FM modulation of the radiofrequency field was used with a modulation amplitude of between 100 and 200 kHz to ensure maximum ENDOR signals without serious line-broadening. No field modulation was used. The modulated radiofrequency was amplified by an ENI Model A300 power amplifier and driven through the ENDOR coil, terminating in a 50-Ω dummy load. Temperature was controlled by either a Bruker ER 4111 VT flowing nitrogen variable temperature accessory or an Oxford EPR-9 liquid helium variable temperature system.

2.3. ENDOR simulations. The complexity of the ENDOR spectra required computer simulations to yield accurate data on the anisotropic hyperfine coupling matrices. The program we developed for this purpose simulates proton ENDOR for the case of isotropic electronic Zeeman interaction (a good approximation here) with all nuclear resonances ($\Delta m_I = \pm 1$) contributing to the ENDOR spectrum. The latter condition implies that cross-relaxation times are much shorter than the electronic spin–lattice relaxation time; independent electron spin echo (ESE) spectroscopy measurements confirm that this condition is satisfied.

The method employed is based on the approach of Dalton and Kwiram (*15*). Given a specific orientation of the external magnetic field with respect to the molecular fixed axes, the program computes transition frequencies from perturbation theory expressions for the energy levels. Nuclear transition moments are evaluated from the wavefunctions for the spin states including the first-order perturbation corrections. The nuclear transition moments are incorporated, together with an empirical saturation parameter to allow for the relaxation effects responsible for ENDOR, into the expression given by Dalton and Kwiram for relative ENDOR intensities. These single-orientation results are then summed over an approximately uniform distribution of orientations over one octant of a sphere to produce a composite stick spectrum on a discrete radiofrequency grid. Finally, a lineshape is convoluted with the spectrum.

The program requires that the user spec-

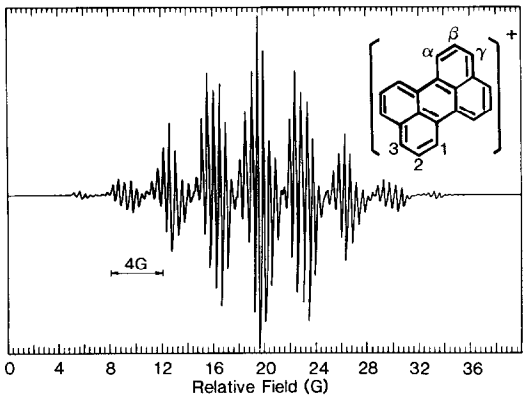

FIG. 2. EPR spectrum of the perylene cation radical formed in concentrated sulfuric acid at room temperature. The four α protons and four γ protons have coupling constants of similar magnitude, $|A_\alpha| = 8.7$ MHz and $|A_\gamma| = 11.5$ MHz, which results in nine groups of lines. These groups are in turn split by the smaller coupling constant of the four β protons, $|A_\beta| = 1.29$ MHz. (Since A_α and A_γ are not identical, A_β splits each group into more than the expected five lines.)

ify (1) the magnetic field employed in the experiment; (2) a value related to the saturation parameter, $S = \gamma_N^2 h_2^2 T_{1N} T_{2N}/2$; and (3) the number of magnetically inequivalent nuclei. Then for each unique nucleus one specifies the principal values of the hyperfine matrix, a lineshape function and a linewidth. The angular intervals, $\Delta\theta$ and $\Delta\phi$, to be used in the summation over orientations are also set by the user. Variables are adjusted until one is satisfied that the best fit has been obtained.

3. RESULTS

Figure 2 shows an X-band EPR spectrum of perylene cation radical, pery(+), in a room temperature solution of concentrated sulfuric acid. The three chemically inequivalent sets of protons, designated α, β, and γ, have isotropic hyperfine coupling constants of $|A_\alpha| = 8.7$ MHz, $|A_\beta| = 1.29$ MHz, and $|A_\gamma| = 11.5$ MHz as measured by simulating the experimental spectrum with programs developed by Belford and coworkers (*19*). In contrast, Fig. 3 shows the EPR spectrum of the radical formed when a 0.001 M solution of perylene in benzene contacts freshly calcined alumina powder. The EPR spectra of this radical on alumina and silica–alumina show no appreciable variation in linewidth over a wide microwave frequency range (L-band (~1.4 GHz), X-band (~9 GHz), and Q-band (~35 GHz)).

Figure 4 shows X-band ENDOR spectra of the perylene radical formed on an alumina surface exposed to ~0.002 M perylene in benzene or d_6-benzene. At 180 K,

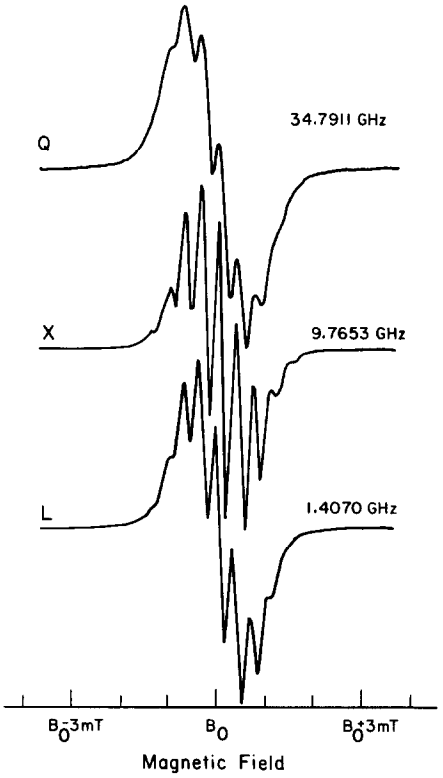

FIG. 3. EPR spectra of the perylene cation radical prepared by injection of a 0.001 M solution of perylene in benzene onto an activated alumina surface. All spectra were run at room temperature within 6 h of sample preparation and are shown with equal magnetic field sweep widths about the g-center, $g = 2.0026$. Operating parameters are as follows, Q-band: mod. amp. = 0.1 G, time cnst. = 30 ms, power = 0.5 mW, freq. = 34.7911 GHz, mag.field at g-center = 12,413 G, sweep rate = 0.42 G/s, one scan. X-band: mod. amp. = 0.1 G, time const. = 20 ms, power = 1.0 mW, freq. = 9.7653 GHz, mag.field at g center = 3484.1 G, sweep rate = 0.5 G/s, two time-averaged scans. L-band: mod.amp. = 1.0 G, time cnst. = 100 ms, power = 1.0 mW, freq. = 1.4070 GHz, mag.field estimated at g-center = 502 G, sweep rate = 0.42 G/s, one scan.

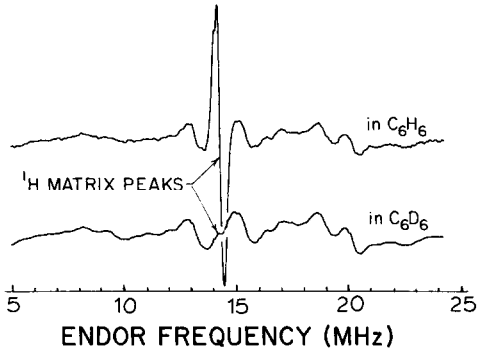

FIG. 4. Comparison of ENDOR spectra of the perylene cation radical prepared by injection of 0.002 M solution of perylene in benzene and d_6-benzene, respectively, onto activated alumina surface. Both spectra obtained from irradiating in center of EPR spectrum at 180 K. Operating parameters, adjusted for optimum signal/noise on existing features in each spectrum, are: microwave power = 5 mW (spectrum in C_6H_6), = 10 mW (spectrum in C_6D_6); rf power maximum (at amplifier meter) = 300–350 W; modulation depth = 150 MHz (spectrum in C_6H_6), = 200 MHz (spectrum in C_6D_6); ENDOR sweep rate = 1.25 MHz/s; time cnst. = 50 ms; 25 time-averaged scans minus an off-resonance background of an additional 25 scans.

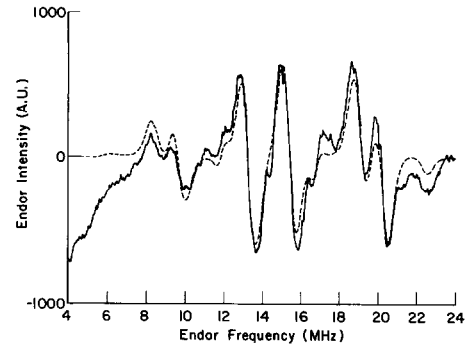

FIG. 5. Comparison of ENDOR spectrum and computer simulation for perylene cation radical prepared by injection of 0.002 M solution of perylene in d_6-benzene onto activated alumina surface. ENDOR spectrum obtained from irradiating in the center of EPR spectrum at 180 K. Operating parameters: microwave power = 10 mW, rf power maximum (at amplifier meter) = 300–350 W, modulation depth = 200 MHz, ENDOR sweep rate = 1.25 MHz/s, time cnst. = 50 ms, 25 time-averaged scans minus an off-resonance background of an additional 25 scans. Simulation parameters: A_{ij} values as listed in Table 1; Gaussian lineshape with full width at half-height values of $\Delta\nu_{1/2}(\alpha) = \Delta\nu_{1/2}(\beta) = 0.6$ MHz, $\Delta\nu_{1/2}(\gamma) = 0.7$ MHz, $S = 0.2$.

the undeuterated sample shows one strong resonance line at about 14.3 MHz (the proton matrix peak) superimposed on a background of weak features spanning the range ~4–24 MHz. In the deuterated sample, most of the proton matrix peak is suppressed, while the former background features remain and can be amplified for careful study (Fig. 5). We attribute these features to the powder-type ENDOR spectrum of the pery(+) protons and interpret through the simulations; see Fig. 5 and Discussion below. Figure 6 shows a similar ENDOR spectrum and simulation for the perylene radical formed on an activated silica–alumina powder (Houdry M-46) exposed to 0.001 M perylene in d_6-benzene. The Houdry M-46 specimens produced much stronger ENDOR spectra than corresponding alumina samples.

ENDOR spectra similar to those shown in Figs. 4–6 were obtained over the temperature range 4 to 180 K. Above that range,

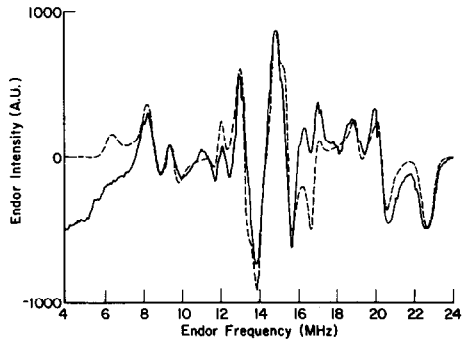

FIG. 6. Comparison of ENDOR spectrum and computer simulation for perylene cation radical prepared by injection of 0.001 M solution of perylene in d_6-benzene onto activated silica–alumina surface. ENDOR spectrum obtained from irradiating in center of EPR spectrum at 110 K. Operating parameters: microwave power = 8 mW, rf power maximum (at amplifier meter) = 300–350 W, modulation depth = 150 MHz, ENDOR sweep rate = 1.5 MHz/s, time cnst. = 50 ms, 25 time-averaged scans minus an off-resonance background of an additional 25 scans. Simulation parameters: A_{ij} values as listed in Table 1; Gaussian lineshape with full width at half-height values of $\Delta\nu_{1/2}(\alpha) = \Delta\nu_{1/2}(\beta) = 0.45$ MHz, $\Delta\nu_{1/2}(\gamma) = 0.7$ MHz, $S = 0.1$.

ENDOR intensity decreased rapidly. The matrix features were accentuated at low temperatures. Only modest variations in lineshape and intensity occurred in the pery(+) proton ENDOR features over the 4 to 180 K range.

4. DISCUSSION

Owing to the motional averaging of anisotropic interactions, the liquid solution (Fig. 2) EPR spectrum of pery(+) shows well-resolved hyperfine structure. The isotropic $|A_{\alpha,\beta,\gamma}|$ values agree well with those reported by others for pery(+) formed chemically in sulfuric acid (*20*) or electrolytically in a solvent mixture (*21*).

The EPR spectra of the adsorbed species (see, for example, Fig. 3) show much lower resolution because of the line-broadening mechanisms discussed in Section 1.2 (e.g., adsorbate/surface interactions, anisotropic hyperfine terms). For radicals such as perylene, one expects g anisotropies of less than 0.1%. These small anisotropies can affect the EPR spectra slightly (*15, 22*). Such EPR spectra have been interpreted previously as if the three proton hyperfine constants were also isotropic (see, e.g., Refs. (*23, 24*)). However, we can expect (*5, 22*) the proton dipolar coupling with electron spin density on the aromatic ring to produce large anisotropy in A for each proton type. This anisotropy contains much valuable information about the nature of the radical and its environment but is largely obscured by line-broadening of the EPR spectrum. The third and weakest (β) proton hyperfine interaction is totally unresolved.

The ability to perform the EPR experiment at different frequencies is important, as a recent review demonstrates (*25*). One unique advantage that it affords is the opportunity to vary the relative importance of terms in the spin Hamiltonian given in Eq. [1]. Higher frequencies (and, hence, higher fields) accentuate field-dependent terms like the electronic Zeeman interaction; lower frequencies give proportionally greater importance to field-independent terms like the hyperfine interaction. In the case of perylene radicals on alumina (Fig. 3) and silica–alumina, the near-invariance of spectral linewidth and of measured g value over a 25-fold microwave frequency range (see Section 3) implies that the g-tensor for this radical is, as expected, not very anisotropic, and that the observed lines are only slightly broadened by frequency-dependent mechanisms such as g-strain.

The usual inability of EPR to resolve weak and anisotropic hyperfine interactions in the spectra of organic radicals in nonoriented samples (powders, polycrystalline samples, glasses) led Hyde *et al.* to perform the first successful ENDOR experiment on a frozen solution containing the triphenylmethyl radical (*18*). Subsequent developments in both instrumentation and theory have made it possible to obtain the information usually obscured in broadened EPR lines by means of ENDOR spectroscopy with simulation, as illustrated in this work in Figs. 4–6. For the perylene radical on alumina and silica–alumina catalysis, the information lost in broadened EPR linewidths is critical for species identification and a study of adsorbate/substrate interactions.

The strong resonance near 14 MHz (Fig. 4) is the result of weak dipole–dipole coupling between the unpaired electron and distant protons. This proton matrix line arises principally from an interaction between the unpaired electron and the solvent protons, although protons attached to the alumina surface can also contribute to its intensity. Deuteration of the solvent to eliminate its contributions to the proton matrix peak should leave just the surface protons, including those of neighboring adsorbates, as the sole contributors to the 14-MHz line; Fig. 4 confirms this expectation.

At first glance, the intramolecular ENDOR spectrum of the perylene radical on

either alumina (Fig. 5) or silica–alumina (Fig. 6) consists of three strong pairs of lines, each pair centered on the 14-MHz free-proton frequency, plus additional weaker features. A superficial interpretation is that the three line pairs correspond to the three pery(+) proton types (α, β, γ or 1, 2, 3) and that the weaker features arise from other species. However, careful study of the behavior of these spectra as functions of sample preparation and conditions as well as spectroscopic variables has convinced us that the aforementioned weaker features are clearly associated with the three pairs of stronger lines because they always maintain their relative positions and intensities.

Having concluded that all the intramolecular ENDOR features of the surface species are part of the same spectrum and having no reason to believe that a perylene radical adsorbed on a disordered oxide surface would be isotropic, we attribute the complexity of the spectrum to complications of anisotropy in the hyperfine coupling interactions of the perylene ring protons. Accordingly, the anisotropic powder-type spectra are interpreted by the computer simulation methods described above (Section 2.3). Fortunately, small g anisotropies affect ENDOR much less than they affect EPR spectra. Thus, the isotropic g assumption in our simulation program is fully justified. The spectral fits shown in Figs. 5 and 6 required many cycles of refinement; Table 1 reports the parameters from the best fits. Apparently, proton hyperfine interaction in this perylene radical on alumina or silica–alumina is quite anisotropic. As Table 1 also shows, the large anisotropy for each proton is in good agreement with the expected dipolar coupling between the proton and the p_π spin density on the nearby carbon atoms (*22*).

The ENDOR spectral simulation is very sensitive to the choice of A_{ij}, and best fits contain an uncertainty in the terms of about ± 0.1 MHz. In order to improve the fit of intensities, the simulation contains a small admixture of a more nearly isotropic spectrum. This ad hoc correction may be necessary because of the degree of surface mobility possessed by radicals in this system. Only line intensities are affected by the correction (lineshapes and positions do not require correction). We currently are studying the sensitivity of ENDOR line intensities to temperature-controlled surface mobility in an effort to better understand this effect.

The substrate composition (alumina vs silica–alumina (Houdry M-46)) had some effect on the ENDOR spectral shape (compare Figs. 5 and 6), attributable to very small differences of anisotropic hyperfine coupling parameters. That the A_{ij}'s derived from the spectra of perylene radicals formed on alumina and silica–alumina are nearly the same strongly suggests that the radical species formed on the two catalysts are identical.

To provide a perspective on just how sensitive the hyperfine coupling constants in this system are to differences between cation and anion and to variations in the interaction between the radical and the surface, Table 1 gives the *isotropic* proton hyperfine constants for perylene cation radicals in different fluid solvents, as well as values for the anion radical. The average values, $\langle |A| \rangle \equiv (|A_{xj}| + |A_{yj}| + |A_{zj}|)/3$, from our data are also shown for both substrates; they indicate the isotropic part ($|A_{\mathrm{iso},j}| = |A_{xj} + A_{yj} + A_{zj}|/3$) *if* all three diagonal components of $\mathbf{A}_j$ have the same sign (a credible assumption for α and γ protons). We see that all proton hyperfine constants in the perylene radicals are sensitive to the molecular environment. Although it is possible that the species we are observing on alumina and silica–alumina is a perturbed anion radical, the hyperfine values we have measured are in better agreement with those measured by ENDOR for the cation in solution (*26, 27*). Also, the extent to which environmental effects can change and α and γ interactions is at this time unknown, but a very signifi-

TABLE I

Proton Hyperfine Coupling for Perylene Radicals (in MHz)

Proton	State	$\lvert A_x \rvert$	$\lvert A_y \rvert$	$\lvert A_z \rvert$	$\langle \lvert A \rvert \rangle$ or A_{iso}	Comments
γ	S = Si/Alu	4.7	12.2	16.7		This work, ENDOR,[a] Houdry M-46 surface
	A = Alu	4.8	12.2	16.8		This work, ENDOR,[a] Act'd alumina surface
	Av, S&A	4.75	12.2	16.75	11.2	This work, average
	Theory[b,c]	−6.0	−11.7	−15.9	−11.2[b]; −12.4[c]	Refs. (*22*, *26*)
	Liq. sol. (+)				−11.44	TRIPLE, cation in liquid TFA[c]
	Liq. sol. (−)				9.8	ENDOR, anion in ion pair in DME[d]
β	S = Si/Alu	0.9	2.3	4.8		This work, ENDOR,[a] Houdry M-46 surface
	A = Alu	1.0	2.3	4.8		This work, ENDOR,[a] Act'd alumina surface
	Av, S&A	0.95	2.3	4.8	2.7	This work, average
	Theory[b,c]	−.3	+2.9	+4.5	+2.4[b]; +4.1[c]	Refs. (*22*, *26*)
	Liq. sol. (+)				+1.26	TRIPLE, cation in liquid TFA[c]
	Liq. sol. (−)				1.2	ENDOR, anion in ion pair in DME[d]
α	S = Si/Alu	5.2	9.7	12.6		This work, ENDOR,[a] Houdry M-46 surface
	A = Alu	5.35	9.7	12.6		This work, ENDOR,[a] Act'd alumina surface
	Av, S&A	5.28	9.7	12.6	9.2	This work, average
	Theory[b,c]	−5.4	−9.9	−12.2	−9.2[b]; −8.7[c]	Refs. (*22*, *26*)
	Liq. sol. (+)				−8.6	TRIPLE, cation in liquid TFA[c]
	Liq. sol. (−)				8.6	ENDOR, anion in ion pair in DME[d]

[a] Experimental values are best fits, by Dalton/Kwiram theory (*15*) simulated for 2025 angular zones, to our experimental ENDOR data for perylene adsorbed on Houdry M-46 (S, silica–alumina) and alumina (A) at 110 K. Signs not determined. Axes (x, y, z) are local, different for each proton, not determined.

[b] Rudimentary theoretical calculations (*22*) based on SCF-MO π-electron spin densities; values for cation radical.

[c] TRIPLE data, pery(+) solution in trifluoroacetic acid, signs determined (*26*), with INDO calculation (*26*).

[d] ENDOR data for liquid solution of Na(+)pery(−) in dimethoxyethane, signs not determined (*27*).

cant perturbation would be needed to cause the anion radical of perylene to exhibit the values of $\lvert A_\alpha \rvert$ and $\lvert A_\gamma \rvert$ which we have measured. For these reasons, we conclude that on the particular alumina and silica–alumina used in this study, the radical formed is the cation.

5. SUMMARY AND CONCLUSIONS

The proton ENDOR spectrum of radicals formed when a solution of perylene in benzene contacts an activated alumina powder in the presence of oxygen contains a complex pattern of intramolecular resonances

of the ring protons overlaid with an intense intermolecular matrix peak, which is enabled by dipolar coupling between the unpaired electron and the more distant protons. Use of fully deuterated solvent to almost totally suppress the matrix line permits detailed study of the weaker intramolecular spectrum, which is considerably more complicated than that expected from purely isotropic hyperfine interactions. Indeed, it is entirely predictable that the expected dipolar coupling between each ring proton and the π spin density on its adjacent carbon atom would produce anisotropic hyperfine coupling as large as the isotropic part; quantitative theoretical predictions (*22*) agree surprisingly well with experimental **A** matrix elements which we have obtained by simulating the intramolecular ENDOR spectra for three chemically distinct types of protons in the molecule. Thus we conclude that the complexity of the ENDOR spectrum is fully accounted for by the anisotropic hyperfine model for a single symmetrical perylene radical species and we reject the superficial interpretation of spectral contributions from multiple species.

Because all nine components of the ring proton hyperfine coupling matrices proved virtually independent of substrate, we infer that *the same* perylene radical was formed on *the particular activated alumina preparation* we used as that which was used on the Houdry M-46 silica–alumina. The following points support assignment of that radical as the cation, pery(+): (1) the literature shows no controversy on the identification of the perylene species on silica–alumina as the cation, (2) the averages of the $|A|$ components for each proton agree better with the isotropic A values for pery(+) in liquid solution (*26*) than for pery(−) (*27*), (3) theoretical predictions (*22*) of the nine hyperfine components for pery(+) are close to the corresponding experimental values. Because the surface chemistry of perylene on alumina is quite dependent on sample composition, crystalline modification (e.g., γ vs η forms), activation conditions, mode of perylene introduction, and subsequent sample treatment, we warn against untested extension of our conclusions. Further work is under way to determine the effects of some of the above-named variables. Section 1.1 cited several mechanisms that have been proposed to explain poor EPR spectral resolution in such systems. If the only species contributing to those spectra is the one we observed and analyzed by ENDOR, then a combination of hyperfine anisotropy, surface immobilization to produce the dispersion of spectral features characteristic of powders, and inhomogeneous line-broadening are the most likely causes of poor EPR resolution. Variations in surface mobility and sample preparation, with their concomitant effects on spectroscopic parameters, including inhomogeneity, could account for sample-to-sample variations in resolution; changes in surface mobility with aging could alter resolution over time in a single sample. Certainly, our data, revealing only three chemically distinct protons in only one species, cannot support suggestions that multiple species with comparable surface concentrations but diverse symmetries exist in our samples.

ACKNOWLEDGMENTS

This research is supported by grants from the U.S. Department of Energy (DOE DEFG 22-84PC70782, Pittsburgh Energy Technology Center); Illinois Department of Energy and Natural Resources, Coal Development Board, through CRSC; and U.S. National Institutes of Health (RR01811, Division of Research Resources). We gratefully acknowledge cooperation in the performance of experiments by Professor Peter G. Debrunner (Physics Department, University of Illinois at Urbana–Champaign) and helpful discussions with Penny A. Snetsinger and Jeffrey B. Cornelius of this department.

REFERENCES

1. Rooney, A. J., and Pink, R. C., *Proc. Chem. Soc.*, 70 (1961).
2. Brauer, D. M., *Chem. Ind. (London)* 177 (1961); *J. Catal.* **1,** 372 (1962).
3. Hall, W. K. *J. Catal.* **1,** 53 (1962).

4. Dollish, F. R., and Hall, W. K., *J. Phys. Chem.* **71,** 1005 (1967).
5. Muha, G. M., *J. Phys. Chem.* **71,** 633 (1967).
6. Muha, G. M., *J. Phys. Chem.* **74,** 2939 (1970).
7. Muha, G. M., *J. Phys. Chem.* **82,** 1843 (1978).
8. Flockhart, B. D., Scott, J. A. N., and Pink, R. C., *Proc. Chem. Soc.*, 139 (1964).
9. Flockhart, B. D., Scott, J. A. N., and Pink, R. C., *Trans. Faraday Soc.* **62,** 730 (1966).
10. Muha, G. M., *J. Catal.* **58,** 470 (1979).
11. Flockhart, B. D., and Salem, M. A., *J. Colloid Interface Sci.* **103,** 76 (1985).
12. Wozniewski, T., Fedorynska, E., and Malinowski, S., *J. Colloid Interface Sci.* **87,** 1 (1982).
13. Reddoch, A. H., *J. Chem. Phys.* **43,** 225 (1965).
14. Muha, G. H., *Chem. Phys. Lett.* **59,** 267 (1978).
15. Dalton, L. R., and Kwiram, A. L., *J. Chem. Phys.* **57,** 1132 (1972).
16. Flockhart, B. D., *Surf. Defect Prop. Solids* **2,** 69 (1973).
17. Kevan, L., and Kispert, L. D., "Electron Spin Double Resonance Spectroscopy." Wiley, New York, 1976.
18. Hyde, J. S., Rist, G. H., and Eriksson, L. E. G., *J. Phys. Chem.* **72,** *4269* (1968).
19. Liczwek, D. L., Belford, R. L., Pilbrow, J. R., and Hyde, J. S., *J. Phys. Chem.* **87,** 2509 (1983).
20. Carrington, A., Dravnieks, F., and Symons, M. C. R., *J. Chem. Soc.*, 947 (1959).
21. Ohya-Nishiguchi, H., *Bull. Chem. Soc. Japan* **52,** 2064 (1979).
22. Snetsinger, P. A., Cornelius, J. B., Rothenberger, K. S., Belford, R. L., Clarkson, R. B., and Crookham, H. C., submitted for publication.
23. Muha, G. M., *J. Chem. Phys.* **67,** 4840 (1977).
24. Ueda, H., *Bull. Chem. Soc. Japan* **49,** 2343 (1976).
25. Belford, R. L., Clarkson, R. B., Cornelius, J. B., Rothenberger, K. S., Nilges, M. J., and Timken, M. D., "Electron Magnetic Resonance of the Solid State" (J. A. Weil, Ed.). Chemical Institute of Canada, Ottawa, 1986.
26. Makela, R., and Voulle, M., *Finn. Chem. Lett.* **3,** 66 (1984).
27. Heineken, F. W., and Christidis, T. C., *Proc. Congress Ampere 18th* **18,** 503 (1974).